2632 *Chem. Mater.* **2009,** *21,* 2632–2640
DOI:10.1021/cm8033559

CHEMISTRY OF MATERIALS
Article

Surface Structure of $LiNi_{0.8}Co_{0.2}O_2$: a New Experimental Technique Using in Situ X-ray Diffraction and Two-Dimensional Epitaxial Film Electrodes

Kazuyuki Sakamoto,[†] Masaaki Hirayama,[†] Noriyuki Sonoyama,[‡] Daisuke Mori,[†] Atsuo Yamada,[†] Kazuhisa Tamura,[§] Jun'ichiro Mizuki,[§] and Ryoji Kanno*,[†]

[†]*Department of Electronic Chemistry, Interdisciplinary Graduate School of Science and Engineering, Tokyo Institute of Technology, 4259 Nagatsuta, Midori-ku, Yokohama 226-8502, Japan,* [‡]*Graduate School of Engineering, Environmental Technology & Urban Planning, Nagoya Institute of Technology, Gokiso-cho, Showa-ku, Nagoya, 466-8555, Japan, and* [§]*Japan Atomic Energy Agency, Synchrotron Radiation Research Center, Kansai Research Establishment, 1-1-1 Kouto Sayo-cho Sayo-gun, Hyogo, 679-5148, Japan*

Received December 12, 2008. Revised Manuscript Received April 20, 2009

Surface and bulk structural changes in $LiNi_{0.8}Co_{0.2}O_2$ were observed during electrochemical reactions using synchrotron X-ray scattering and a restricted reaction plane of two-dimensional (2D) epitaxial-film electrodes. The bulk structural changes confirmed lithium diffusion through the (110) surface, which is perpendicular to the 2D edges of the layered structure. No (de)intercalation reaction was observed through the (003) surface in the voltage range of 3.0−5.0 V. However, intercalation proceeded below 3.0 V, which indicates unusual three-dimensional lithium diffusion in the 2D structure in the overlithiated state. Structural changes at the electrode surface were different from those in the bulk. Contact with the liquid electrolyte caused an abrupt deformation of the surface crystal lattice, followed by restructuring upon applying a cell voltage. These slow reconstruction processes were dependent on the crystal lattice orientations. The reaction mechanism of the intercalation electrodes for lithium batteries is discussed on the basis of the surface and bulk structural changes that occur during electrochemical reactions.

1. Introduction

Intercalation is a chemical reaction where guest ions are inserted and extracted within gaps in host lattices with no substantial change to the lattice itself. It forms the basis on which lithium batteries function, when the reaction is driven electrochemically.[1−3] Although the lattice change during intercalation is minimal, the restructuring process is often accompanied by a phase transition and is one of the key factors that determine the kinetics and reversibility of lithium batteries.[4−6] Thus, the intrinsic characteristics of battery components can be improved by modifying the bulk materials.[2−9] However, recent electrochemical studies have claimed that the most significant problem associated with the kinetics, reversibility, and long-term stability of battery reactions is the electrode/electrolyte interface.[10,11] High-resolution insight into the interface during electrochemical reactions is a prerequisite for an atomistic understanding and control of kinetics in lithium battery reactions.

Previous structural studies have dealt with bulk crystals, and structural information for the electrode surface, where the reaction is initiated, has been lacking. At the electrode/electrolyte interface, where the potential gradient between two electrodes is accumulated in the very thin electrolyte layer, a series of reactions takes place: lithium diffusion in the electrolyte, adsorption of solvated lithium on the electrode surface, desolvation, surface diffusion, charge-transfer, and intercalation from the surface to the bulk crystal.[10,11] Electrochemical analyses point to desolvation as the rate-determining step in battery reactions among the series of electrochemical reactions taking place at the interface.[10] However, in the absence of detailed information on each reaction, the key factors that determine rate capabilities remain unclear.

Epitaxial-film electrodes offer advantages for mechanistic studies on lithium (de)intercalation and surface structural changes because the two-dimensional (2D) interface

*To whom correspondence should be addressed. E-mail: kanno@echem.titech.ac.jp. Fax: +81-45-924-5409. Phone: +81-45-924-5401.

(1) Tarascon, J. M.; Armand, M. *Nature* **2001**, *414*, 359.
(2) Whittingham, M. S. *Science* **1976**, *192*, 1126.
(3) Mizushima, K.; Jones, P. C.; Wiseman, P. J.; Goodenough, J. B. *Mater. Res. Bull.* **1980**, *15*, 783.
(4) Kanno, R.; Takeda, Y.; Ichikawa, T.; Nakanishi, K.; Yamamoto, O. *J. Power Sources* **1989**, *26*, 535.
(5) Mohri, M.; Yanagisawa, N.; Tajima, Y.; Tanaka, H.; Mitate, T.; Nakajima, S.; Yoshida, M.; Yoshimoto, Y.; Suzuki, T.; Wada, H. *J. Power Sources* **1989**, *26*, 545.
(6) Croguennec, L.; Pouillerie, C.; Mansour, A. N.; Delmas, C. *J. Mater. Chem.* **2001**, *11*, 131.
(7) Gover, R. K. B.; Kanno, R.; Mitchell, B. J.; Yonemura, M.; Kawamoto, Y. *J. Electrochem. Soc.* **2000**, *147*, 4045.
(8) Yamada, A.; Koizumi, H.; Nishimura, S. I.; Sonoyama, N.; Kanno, R.; Yonemura, M.; Nakamura, T.; Kobayashi, Y. *Nat. Mater.* **2006**, *5*, 357.
(9) Kang, K. S.; Meng, Y. S.; Breger, J.; Grey, C. P.; Ceder, G. *Science* **2006**, *311*, 977.
(10) Abe, T.; Fukuda, H.; Iriyama, Y.; Ogumi, Z. *J. Electrochem. Soc.* **2004**, *151*, A1120.
(11) Nakayama, M.; Ikuta, H.; Uchimoto, Y.; Wakihara, M. *J. Phys. Chem. B* **2003**, *107*, 10603.

 Published on Web 05/14/2009

restricts their reaction fields, which could enable the lattice plane dependence of the reaction to be detected directly. Moreover, the flat electrode surface could allow detection of structural changes occurring exclusively at the very surface of the electrode, where the intercalation reaction is initiated.

The present study is the first to examine the surface of the intercalation electrodes directly, using the model electrode $LiNi_{0.8}Co_{0.2}O_2$. The two-dimensionality of our films allow us to restrict the surface planes on which the insertion reaction is initiated: the (110) and (003) orientations correspond, respectively, to the planes perpendicular and parallel to the edges of the 2D-layered structure.[12−14] Direct evidence of lithium diffusion in the layered materials and surface structural changes induced by the interfacial reactions were detected by in situ X-ray diffraction (XRD) and surface X-ray diffraction (SXRD) for layered $LiNi_{0.8}Co_{0.2}O_2$ with ideal 2D flat electrode surfaces of (110) and (003) lattice planes.

2. Experimental Section

The $LiNi_{0.8}Co_{0.2}O_2$ epitaxial film was synthesized by the pulsed laser deposition (PLD) method using the apparatus PLD 3000 (PVD Products, Inc.).[13] The films were deposited on the (110) and (111) planes of the $SrTiO_3$ substrate (0.5 wt % Nb-doped) using a KrF excimer laser with a wavelength of 248 nm under O_2. The deposition conditions were as follows: Li/M ratio = 1.3/1.0; temperature, T = 600 °C; distance between substrate and the target, d = 7.5 cm; laser frequency, f = 10 Hz; deposition time, t = 60 min; laser energy, E = 200 mJ; and pressure, pO_2 = 25 mTorr. The film thickness and roughness determined by X-ray surface reflectometer were about 10 and 0.2 nm, respectively. Thin-film XRD data were recorded by a thin-film X-ray diffractometer (Rigaku ATX-G) with Cu $K\alpha_1$ radiation. The orientation of the films was characterized both by out-of-plane and in-plane measurements.[12−15] The orientation of the lattice planes of $LiNi_{0.8}Co_{0.2}O_2$ was successfully controlled by changing the substrate orientation. $LiNi_{0.8}Co_{0.2}O_2$ (110) and $LiNi_{0.8}Co_{0.2}O_2$ (003) were deposited on $SrTiO_3$ (110) and $SrTiO_3$ (111) substrates, respectively.[13] The $LiNi_{0.8}Co_{0.2}O_2$ (110) film has a surface plane consisting of the 2D edges of the layered structure. The (003) planes are parallel to the 2D edges of the layered structure for the $LiNi_{0.8}Co_{0.2}O_2$ (003) film.

The in situ XRD was measured with a κ-type six-circle diffractometer (New Port) installed on the bending-magnet beamline BL14B1 at SPring-8.[12−15] The X-rays were monochromated by a Si(111) double crystal system and focused by two Rh-coated bent mirrors. The beam size of the incident X-ray was 0.1 mm (vertical) × 0.4−1.0 mm (horizontal), which was adjusted by a slit placed in front of the sample. The angular acceptance of the receiving slit was 2 mrad for the 2θ direction and 20 mrad for the χ direction. A wavelength of 0.82552 Å (15 keV) was selected. The in situ spectro-electrochemical cell designed for our experiments provided continuous structural changes with the electrochemical lithium intercalation and deintercalation.[13−15] An electrolyte solution of EC/DEC with a molar ratio of 3:7 and 1M-$LiPF_6$ was injected into the spectro-electrochemical cell. Deintercalation and intercalation were carried out by the potentiostatic method with a potentiostat/galvanostat (Hokuto Denko, HA-501). Structural changes were observed by the potentiostatic method during the electrochemical (de)intercalation. Once the cell potential stabilized, the electrolyte was poured out from the outlet of the cell until the Mylar window was placed on the surface of the epitaxial film. This thin layer configuration has advantages in avoiding X-ray scattering by the solution. After the XRD measurements, the electrolyte was poured into the cell again, and the cell potential was changed to a fixed value for the next measurement.

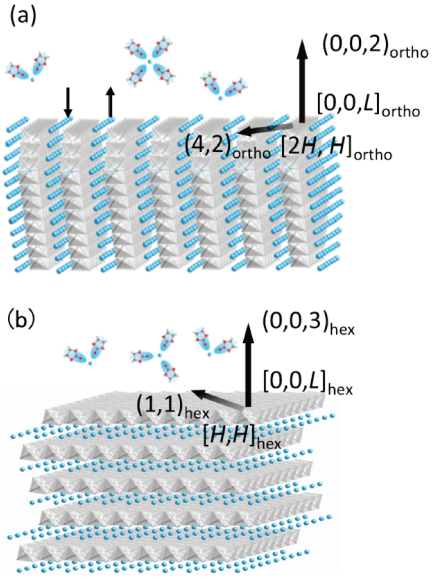

Figure 1. Schematic drawing of $LiNi_{0.8}Co_{0.2}O_2$ (110) (a) and $LiNi_{0.8}Co_{0.2}O_2$ (003) (b).

A reciprocal coordinate system (H, K, L) with two components (H and K) lying parallel to the surface and a third (L) along the surface normal was used (see Figure 1). For the $LiNi_{0.8}Co_{0.2}O_2$(110) epitaxial film, the new reciprocal coordinate system is described by an orthorhombic system, and the relationship between $(H, K, L)_{ortho}$ and $(h, k, l)_{hex}$ for the hexagonal lattice of $LiNi_{0.8}Co_{0.2}O_2$(110) is given by the transformations $H = l$, $K = h - k$, and $L = h + k$. For example, $(1, 1, 0)_{hex} = (0, 0, 2)_{ortho}$ and $(1, -1, 4)_{hex} = (4, 2)_{ortho}$ correspond to bulk and surface reflections, respectively (shown in Figure 1a). The reciprocal orthorhombic lattice parameters of the epitaxial film determined by ex situ XRD measurements, for example, are a^* = 1.2558, b^* = 0.4410, and c^* = 2.1751 Å^{-1}. The $(0, 0, 2)_{ortho}$ and $(4, 1, 1)_{ortho}$ diffraction peaks were measured by the out-of-plane scan, and the $(4, 2)_{ortho}$ and $(6, 0)_{ortho}$ peaks by the in-plane scan. For the $LiNi_{0.8}Co_{0.2}O_2$ (003) epitaxial film, the reciprocal coordinate is described by the same hexagonal lattice. We used the $(0, 0, 3)_{hex}$, $(1, 0, 4)_{hex}$, and $(1, 1)_{hex}$ diffraction peaks, providing the bulk and surface structural changes (shown in Figure 1b). These peak shifts were

(12) Hirayama, M.; Sonoyama, N.; Abe, T.; Minoura, M.; Ito, M.; Mori, D.; Yamada, A.; Kanno, R.; Terashima, T.; Takano, M.; Tamura, K.; Mizuki, J. *J. Power Sources* **2007**, *168*, 493.
(13) Hirayama, M.; Sakamoto, K.; Hiraide, T.; Mori, D.; Yamada, A.; Kanno, R.; Sonoyama, N.; Tamura, K.; Mizuki, J. *Electrochim. Acta* **2007**, *53*, 871.
(14) Sakamoto, K.; Konishi, H.; Sonoyama, N.; Yamada, A.; Tamura, K.; Mizuki, J.; Kanno, R. *J. Power Sources* **2007**, *174*, 678.
(15) Hirayama, M.; Sonoyama, N.; Ito, M.; Minoura, M.; Mori, D.; Yamada, A.; Tamura, K.; Mizuki, J.; Kanno, R. *J. Electrochem. Soc.* **2007**, *154*, A1065.

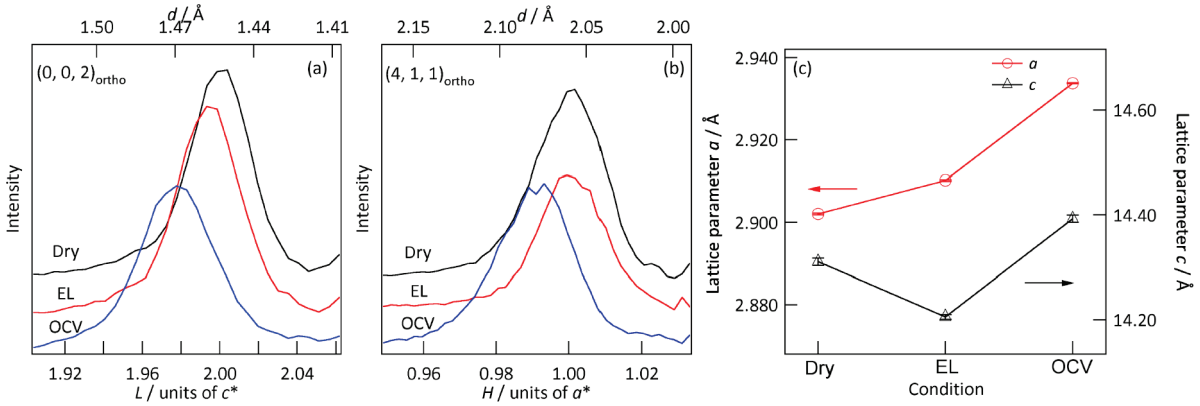

Figure 2. In situ XRD peaks of the $(0, 0, 2)_{ortho}$ (a) and $(4, 1, 1)_{ortho}$ (b), and the lattice parameters (c) for the $LiNi_{0.8}Co_{0.2}O_2$ (110). Dry: pristine sample, EL: after immersed into the electrolyte, OCV: after constructing lithium cell.

observed under different conditions and in a different voltage range. The out-of-plane and in plane diffractions were measured for the pristine sample (Dry), then the electrolyte was injected into the cell, and the diffractions were measured again for the same reflections (EL). The cells were removed from the diffractometer, lithium metal was set in the in situ cell, and the diffraction of the same peaks was measured (OCV). After these initial runs, the diffraction peaks were measured at fixed voltages between 2.0 and 5.0 V.

3. Results and Discussion

3.1. Bulk Structural Changes in (110) Thin Films. Figure 2 shows the in situ XRD peaks of $(0, 0, 2)_{ortho}$ and $(4, 1, 1)_{ortho}$ of the pristine sample (Dry), after the injection of electrolyte (EL) and the construction of a Li cell (OCV). The hexagonal cell parameters calculated from these reflections are also indicated. After the electrode was placed into contact with the electrolyte (EL), the $(0, 0, 2)_{ortho}$ and $(4, 1, 1)_{ortho}$ peaks shifted to higher and lower *d*-values, respectively. In the OCV state, the $(0, 0, 2)_{ortho}$ and $(4, 1, 1)_{ortho}$ peaks shifted to higher *d*-values. Unexpectedly, the bulk structure changed in the initial stage of lithium cell construction, indicating a reaction between the electrode and the liquid electrolyte. Previously, we reported that the surface of the $LiNi_{0.8}Co_{0.2}O_2$ epitaxial film was covered with an impurity phase with a thickness of ~1 nm.[13] The impurity layer had a density of about 2 g cm^{-3} and might be lithium carbonate or lithium hydroxide. The surface of the pristine electrode reacts with the moisture and carbon dioxide in the ambient air with formation of the surface impurity layer. During this process, a lithium-proton exchange and/or a valence change of Ni/Co ions should have occurred in the $LiNi_{0.8}Co_{0.2}O_2$ bulk region. A similar behavior has recently been observed for nanosized $LiFePO_4$ polycrystalline: a small amount of lithium is spontaneously deintercalated upon air exposure.[16] After the sample was soaked in the electrolyte, it is reasonable to assume the lithium diffusion between the electrode and the electrolyte caused by a moderation in concentration gradient of lithium ions and formation of an electrical double layer at the interface. Our in situ thin-film XRD demonstrates the lattice expansion of the $LiNi_{0.8}Co_{0.2}O_2$ bulk (< 25 nm from the surface) after the electrolyte soak, which might be caused by the lithium intercalation during the initial interfacial reactions.

Figure 3 shows the $(0, 0, 2)_{ortho}$ and $(4, 1, 1)_{ortho}$ reflections under an applied cell voltage from OCV (2.96 V) to 5.0 V, and then from 5.0 to 2.0 V. The peak shifted to lower *d*-values with increasing cell voltage from the initial voltage of 2.96 V, and shifted reversibly with decreasing cell voltage from 5.0 V. This indicates reversible intercalation through the edge plane of the 2D structure of $Li_xNi_{0.8}Co_{0.2}O_2$ (110). The lattice parameters, a_{hex} and c_{hex}, shown in Figure 3c, decreased in going from 3.0 to 4.2 V. Polycrystalline $Li_xNi_{0.8}Co_{0.2}O_2$ showed reversible structural changes with rhombohedral symmetry over the composition range of $0.4 \leq x \leq 1.0$,[17] where the *a*- and *c*-axes decreased and increased, respectively, upon anodic polarization.[18−20] While the rhombohedral phase was reported to transform into a new hexagonal phase at $x < 0.2$ in the Li_xNiO_2 system,[19,20] no significant peak splitting was observed for the epitaxial film, which is indicative of the absence of a phase transition. The peaks shifted reversibly as the cell voltage decreased to 3.0 V without peak intensity changes. The close interaction between the electrode and the substrate might restrict the large bulk structural changes during the lithium (de)intercalation process, and cause the small lattice change of the epitaxial $LiNi_{0.8}Co_{0.2}O_2$ (110) film. We should also take into account nanosize effects reported for nanoparticles of the electrode materials. The effects are related to the short diffusion length for lithium ion and electron transfer, large contact area to the electrolyte, and lower physical strains by lithium (de)intercalation.[21,22] These conditions lead the nanosized particles to show larger solid solution region and faster lithium ion diffusion than micrometer-sized

(16) Martin, J. F.; Yamada, A.; Kobayashi, G.; Nishimura, S. I.; Kanno, R.; Guyomard, D.; Dupre, N. *Electrochem. Solid State Lett.* **2008**, *11*, A12.
(17) Davidson, I.; Greedan, J. E.; Vonsacken, U.; Michal, C. A.; Dahn, J. R. *Solid State Ionics* **1991**, *46*, 243.
(18) Saadoune, I.; Delmas, C. *J. Solid State Chem.* **1998**, *136*, 8.
(19) Croguennec, L.; Pouillerie, C.; Delmas, C. *J. Electrochem. Soc.* **2000**, *147*, 1314.
(20) Croguennec, L.; Pouillerie, C.; Delmas, C. *Solid State Ionics* **2000**, 259.
(21) Wagemaker, M.; Borghols, W. J. H.; Mulder, F. M. *J. Am. Chem. Soc.* **2007**, *129*, 4323.
(22) Zhou, H. S.; Li, D. L.; Hibino, M.; Honma, I. *Angew. Chem., Int. Ed.* **2005**, *44*, 797.

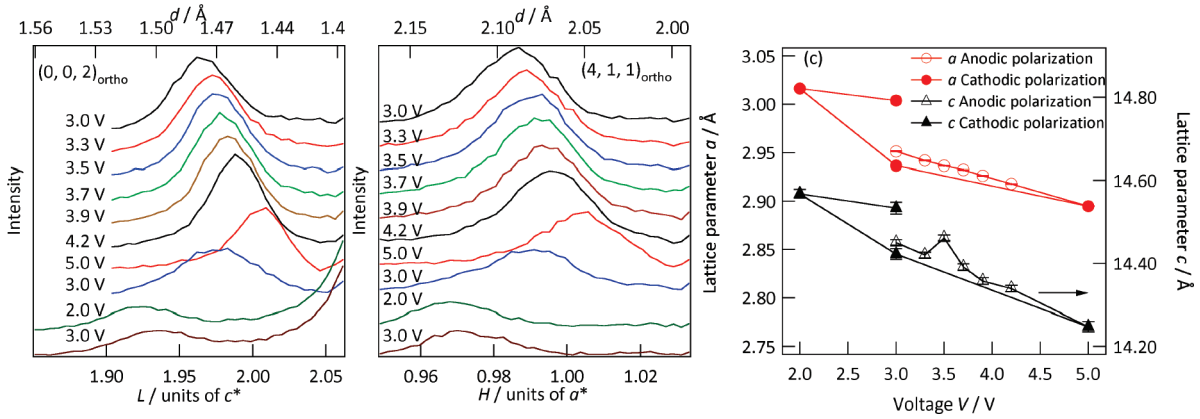

Figure 3. In situ XRD peaks of $(0, 0, 2)_{ortho}$ (a), $(4, 1, 1)_{ortho}$ (b) and voltage dependence of lattice parameters (c) for $LiNi_{0.8}Co_{0.2}O_2$ (110) during anodic potential steps from 3.0 to 5.0 V and cathodic potential steps from 5.0 to 2.0 V.

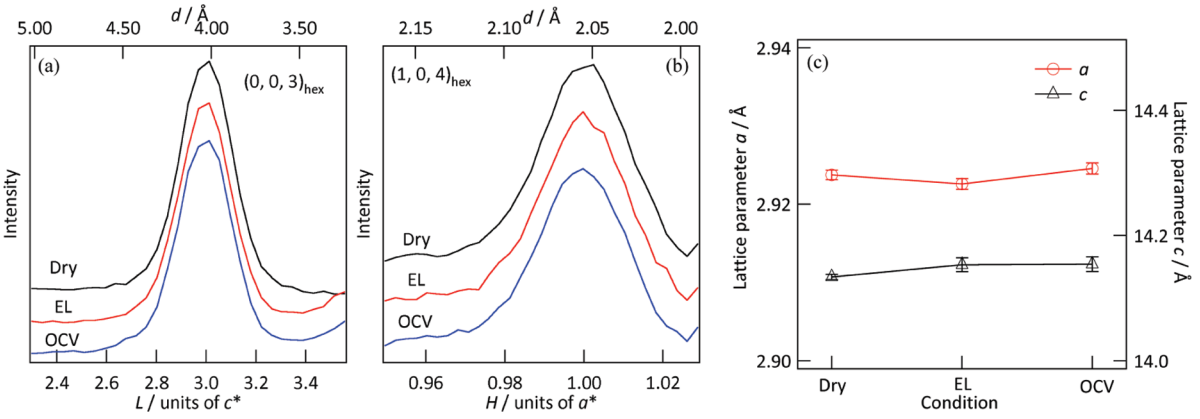

Figure 4. In-situ XRD peaks of $(0, 0, 3)_{hex}$ (a) and $(1, 0, 4)_{hex}$ (b), and lattice parameters (c) for the $LiNi_{0.8}Co_{0.2}O_2$ (003).

particles. The very small thickness of the epitaxial films might cause the single-phase reaction behavior in the bulk region from 3.0 to 4.2 V. In the overlithiated state below 2.0 V, the $(0, 0, 2)_{ortho}$ and $(4, 1, 1)_{ortho}$ peaks largely shifted to lower *d*-values and the a_{hex} and c_{hex} parameters increased with decreasing voltage. These large lattice changes suggest a phase transition from the rhombohedral phase. The overlithiated phase Li_2NiO_2 has been reported to have a hexagonal close packed (h.c.p.) structure with $P\bar{3}m1$ symmetry (Space Group No.164).[23] Similar structural changes have previously been reported for the overlithiated form of Li_2MO_2 (M = Co, Ni, Mn).[24−26] The *d*-value of the $(0, 0, 2)_{ortho}$ reflection for $LiNi_{0.8}Co_{0.2}O_2$ (110) is 1.502 Å, which is consistent with the *d*-value of Li_2NiO_2 (1.550 Å). These results indicate a formation of the hexagonal Li_2MO_2 phase for the $LiNi_{0.8}Co_{0.2}O_2$ (110) film which is accompanied by a transformation of oxygen packing from c.c.p to h.c.p at 2.0 V.

3.2. Bulk Structural Changes in (003) Films. Figure 4 shows the $(0, 0, 3)_{hex}$ and $(1, 0, 4)_{hex}$ diffraction peaks of the pristine samples (Dry) after the injection of electrolyte (EL) and construction of cells (OCV). The absence of peak shift indicates the absence of intercalation reaction through the (003) lattice plane at the initial stage of cell formation. Our previous studies on X-ray reflectometry (XRR) indicated that the surface of the $LiNi_{0.8}Co_{0.2}O_2$ epitaxial film was covered with an impurity phase, Li_2CO_3 or LiOH, formed by a reaction with ambient air, and these films disappeared after the samples were soaked in the electrolyte without forming an SEI layer at the (003) surface.[13] The absence of structural changes in the present study are consistent with the XRR results.

Figure 5 shows the $(0, 0, 3)_{hex}$ and $(1, 0, 4)_{hex}$ reflections and the lattice parameter changes with the electrochemical reactions from 3.0 to 5.0 V and from 5.0 to 2.0 V. Between 3.0 and 5.0 V, no lithium (de)intercalation reaction was observed through the (003) plane parallel to the 2D transition metal layers, which is consistent with the 2D character of the layered materials. However, these peaks shifted to lower *d*-values upon applying voltage from 3.0 to 2.0 V, which indicates lithium intercalation into the structure (Figure 5b,d); lithium penetrates the 2D $[(Ni,Co)O_6]$ layer from the surface and diffuses three-dimensionally in the 2D structure. The *d*-value of the $(0, 0, 3)_{hex}$ reflection for $LiNi_{0.8}Co_{0.2}O_2$ (003) is 4.967 Å, which is almost consistent with the *d*-value (5.090 Å) of the 002 reflection for Li_2NiO_2.[23] Previously we reported a three-dimensional (3D) lithium diffusion in $LiNi_{0.5}Mn_{0.5}O_2$ (003) epitaxial

(23) Davidson, I. J.; Greedan, J. E.; Vonsacken, U.; Michal, C. A.; Mckinnon, W. R. *J. Solid State Chem.* **1993**, *105*, 410.
(24) Johnson, C. S.; Kim, J. S.; Kropf, A. J.; Kahaian, A. J.; Vaughey, J. T.; Fransson, L. M. L.; Edstrom, K.; Thackeray, M. M. *Chem. Mater.* **2003**, *15*, 2313.
(25) David, W. I. F.; Goodenough, J. B.; Thackeray, M. M.; Thomas, M. *Rev. Chim. Miner.* **1983**, *20*, 636.
(26) Benedek, R.; Vaughey, J.; Thackeray, M. M. *Chem. Mater.* **2006**, *18*, 1296.

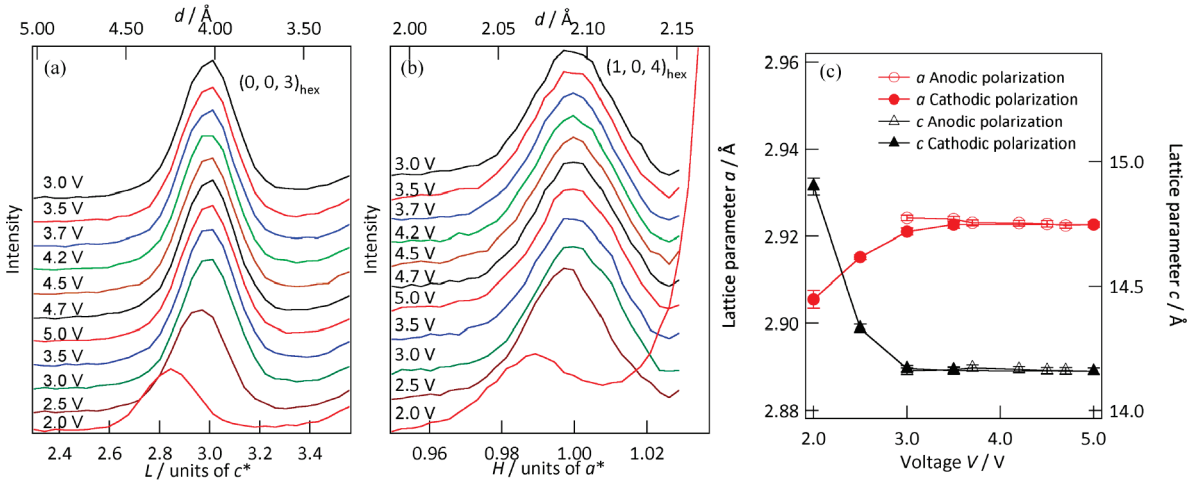

Figure 5. In-situ XRD peaks of $(0, 0, 3)_{hex}$ (a), $(1, 0, 4)_{hex}$ (b), and voltage dependence of lattice parameters (c) for the $LiNi_{0.8}Co_{0.2}O_2$ (003) during anodic potential steps from 3.0 to 5.0 V and anodic polarization from 5.0 to 2.0 V.

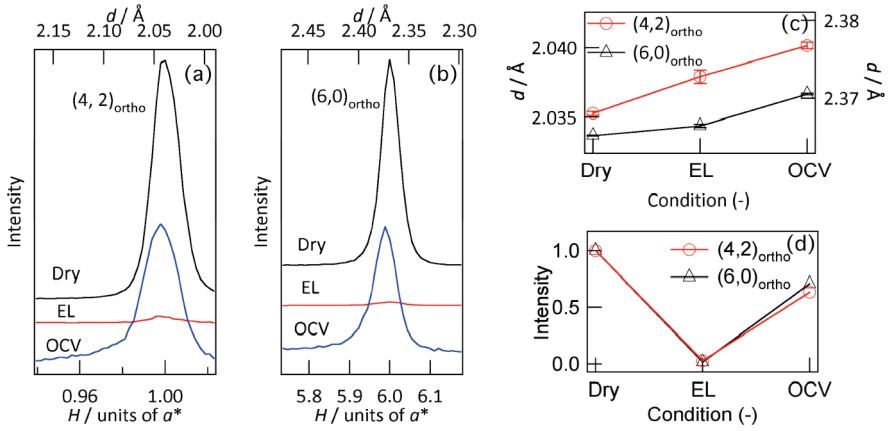

Figure 6. Surface XRD peaks of $(4,2)_{ortho}$ and $(6,0)_{ortho}$ and *d*-values for $LiNi_{0.8}Co_{0.2}O_2$ (110).

thin-film with a large amount of cation mixing at both the lithium and the metal sites.[14] Lithium diffusion through the transition metal layer was also reported for the polycrystalline $LiNi_{0.5}Mn_{0.5}O_2$ which contains a small amount of Li at the transition metal layer, and the Li at the transition metal layer participates in the lithium diffusion.[27,28] These studies indicate the 3D lithium ion diffusion in the 2D layer structure. However, our results on $LiNi_{0.8}Co_{0.2}O_2$ (003) indicate no lithium diffusion at the higher voltage region between 3.0 and 4.2 V, while the lithium diffusion was observed below the 3 V region. This result suggests that the 3D diffusion mechanism might be different from that of the $LiNi_{0.5}Mn_{0.5}O_2$ reported previously. The possible explanation of the 3D diffusion in the 2D structure might be based on the structural transformation at this voltage region. As indicated by the polycrystalline materials, the oxygen packing of the structure changes from c. c. p. to h. c. p. at this voltage region, which is also observed for our epitaxial (110) film electrodes. The displacement of the oxygen packing along the *c* plane might cause an unusual lithium diffusion perpendicular to the displacement plane.

3.3. Surface Structural Changes in (110) Films. Figure 6 shows the in-plane diffraction peaks, $(4, 2)_{ortho}$ and $(6, 0)_{ortho}$, of the epitaxial $LiNi_{0.8}Co_{0.2}O_2$(110) film electrode under the Dry, EL, and OCV conditions. The peak intensities decreased dramatically after the electrode was immersed in the electrolyte and increased again under the OCV condition. The peak shifted to a higher *d*-value in going from the Dry to the OCV state. Although X-ray adsorption of the electrolyte caused a decrease in the intensities, the re-increase in intensity point to surface structural changes during the initial cell construction process. A restructuring process followed the collapse of the surface structure because of reactions between the electrode surface and electrolyte. The increase in *d*-values is indicative of a reaction between the surface crystal lattice and the electrolyte that causes changes in compositions and the valence of transition metals.

The intensity changes in the surface reflections were accounted for by a shift of transition metals at the surface according to the following conditions: (i) the reaction between the surface and electrolyte might cause rearrangement of the surface crystal lattice, (ii) the X-ray intensity is

(27) Arachi, Y.; Kobayashi, H.; Emura, S.; Nakata, Y.; Tanaka, M.; Asai, T.; Sakaebe, H.; Tatsumi, K.; Kageyama, H. *Solid State Ionics* **2005**, *176*, 895.
(28) Yoon, W. S.; Paik, Y.; Yang, X. Q.; Balasubramanian, M.; McBreen, J.; Grey, C. P. *Electrochem. Solid-State Lett.* **2002**, *5*, A263.

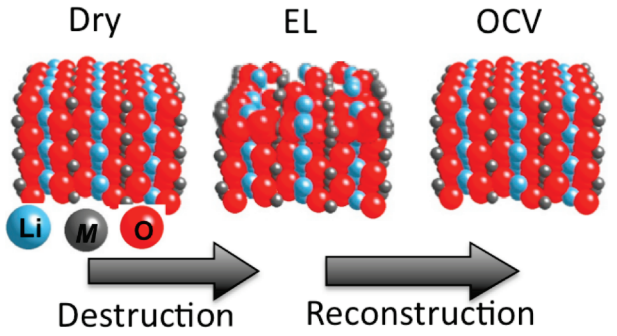

Figure 7. Schematic drawing of $LiNi_{0.8}Co_{0.2}O_2$ (110). The surface destructed after soaked into electrolyte (EL), and reconstruction proceeds at the OCV state.

mainly due to the heavy transition metals, and (iii) the surface crystal arrangement is restricted by the symmetry of the bulk crystal structure. The intensities of the $(4, 2)_{ortho}$ and $(6, 0)_{ortho}$ diffraction peaks were then calculated on the basis of a rhombohedral system (Space group: $R\bar{3}m$): with the lithium at 3*a* (000), nickel/cobalt at 3*b* (001/2), oxygen atoms occupy the 6*c* (00*z*) site with $z = 0.27$.[13] Site splittings of the transition metal 3*b* site were considered: 18*g* (*x*01/2) ($x = 0-0.01$), 6*c* (00*z*) ($z = 0-0.01$), and 36*i* (*xyz*) (x, $z = 0-0.01$, $y = 0$) sites. Among the models considered, the intensities of the $(4, 2)_{ortho}$ and $(6, 0)_{ortho}$ diffraction peaks showed minimum values at $x = 0.001$ and $z = 0$ with the 18*g* site, and the peak intensity changes were consistent with the measured diffraction peak intensity changes. According to the model, the transition metal ions shifted along the ⟨110⟩ direction at the surface. These structural changes might be expected after the electrolyte soak. The metal position shifted again at the OCV state (see Figure 7). Changes in adsorption species and/or ion diffusion at the electrode surface may be responsible for the surface deconstruction observed after the electrolyte soak, followed by a reconstruction at the OCV state. The reconstructed structure might be different from the original structure before the initial reaction because of the different ambient conditions, in the air or electrolyte. This is the first example of an active electrode surface behaving differently from the bulk structure, previously characterized only by lattice expansion and shrinkage with lithium (de)intercalation. It is widely recognized that surface restructuring is caused by chemical adsorption of gas species on the clean surface of semiconductors, and the restructuring mechanism is studied extensively by a wide variety of experimental techniques under vacuum.[29] Although a similar process was observed for under-potential deposition (UPD) on single crystal electrodes,[30] no such phenomena have been found in the case of materials for electrochemical devices such as lithium batteries. Our results of surface restructuring on the intercalation electrode are quite similar to those observed for the clean surface of semiconductors. Figure 8 shows the diffraction peaks $(4, 2)_{ortho}$ and $(6, 0)_{ortho}$, and their *d*-values change with applied voltage from OCV to 5.0 V, and to 2.0 V. The $(6, 0)_{ortho}$ peak shifted to lower *d*-values with increasing voltage from 3.0 to 5.0 V, as in the case of the bulk structure. However, a new peak appeared next to the $(4, 2)_{ortho}$ peak from 3.5 V. This might be caused by a two-phase domain at the crystal surface or symmetry reduction only at the lattice plane. For example, these peaks could be indexed as $(-2, 0)_{mono}$ and $(-3, 2)_{mono}$ if a symmetry change from rhombohedral to monoclinic is assumed. Although the reason for the splitting remains clear, the structural change behavior at the surface is different from that in the bulk. Below 3.0 V, the *d*-values increased dramatically, which is strongly influenced by the bulk structural change from the c. c. p. to the h. c. p. arrangement for the overlithiated phase.

3.4. Surface Structural Changes in (003) Films. Figure 9 shows the $(1,1)_{hex}$ peak of the Dry, EL, and OCV conditions. The intensities and *d*-values of these peaks are also indicated. The $(1,1)_{hex}$ reflection was measured along the $[H,H]_{hex}$ direction of the reciprocal coordinate system. The data are plotted as a function of *H* and *d*-value. Although no peak shift was observed for the (003) film, the peak intensities decreased dramatically after the electrode was attached to the electrolyte and increased slightly under the OCV condition, indicating a surface structural change at the initial process. This is similar to the behavior observed for the (110) surface.

Figure 10 shows the voltage dependence of the peak profile and *d*-values of the $(1,1)_{hex}$ peak with anodic polarization steps from 3.0 to 5.0 V and cathodic steps from 5.0 and 2.0 V. No changes were observed in the *d*-values for the potential range of 3.0−5.0 V, as expected from the 2D nature of the structure. Although a small change in the *d*-value was observed at 2.0 V, there was no change in peak intensity. The surface structural changes in the (110) films could be related to the lithium intercalation process because reversible lithium (de)intercalation was observed only through the edge plane of the 2D structure of $LiNi_{0.8}Co_{0.2}O_2$ (110). The absence of lithium (de)intercalation for the (003) plane is consistent with the absence of surface structural changes in the (003) electrode above 3.0 V.

3.5. Surface Reactions at the $LiNi_{0.8}Co_{0.2}O_2$ Electrode. Most previous studies on the electrode surface of $LiNiO_2$-based materials were based on ex situ techniques using polycrystalline materials. As for surface impurity phases, Li_2CO_3 was detected on the $LiNi_{0.81}Co_{0.16}Al_{0.03}O_2$ surface after exposure to air,[31] and $LiNiO_2$ would chemically delithiate without electron exchange, for example, by reacting with H_2O.[32] These results pointed to an interfacial reaction with the moisture or CO_2 in air, leading to the formation of an impurity phase at the electrode surface. During the first electrochemical reaction, the $LiNi_{0.8}Co_{0.2}Al_{0.05}O_2$ electrode surface was analyzed by ex situ Fourier transform IR spectroscopy in the EC/DEC-1M$LiPF_6$ electrolyte.[33] No reactions were observed below

(29) Schlier, R. E.; Farnsworth, H. E. *J. Chem. Phys.* **1959**, *30*, 917.
(30) Wang, J.; Davenport, A. J.; Isaacs, H. S.; Ocko, B. M. *Science* **1992**, *255*, 1416.
(31) Matsumoto, K.; Kuzuo, R.; Takeya, K.; Yamanaka, A. *J. Power Sources* **1999**, *82*, 558.
(32) Moshtev, R.; Zlatilova, P.; Vasilev, S.; Bakalova, I.; Kozawa, A. *J. Power Sources* **1999**, *82*, 434.
(33) Song, S. W.; Zhuang, G. V.; Ross, P. N. *J. Electrochem. Soc.* **2004**, *151*, A1162.

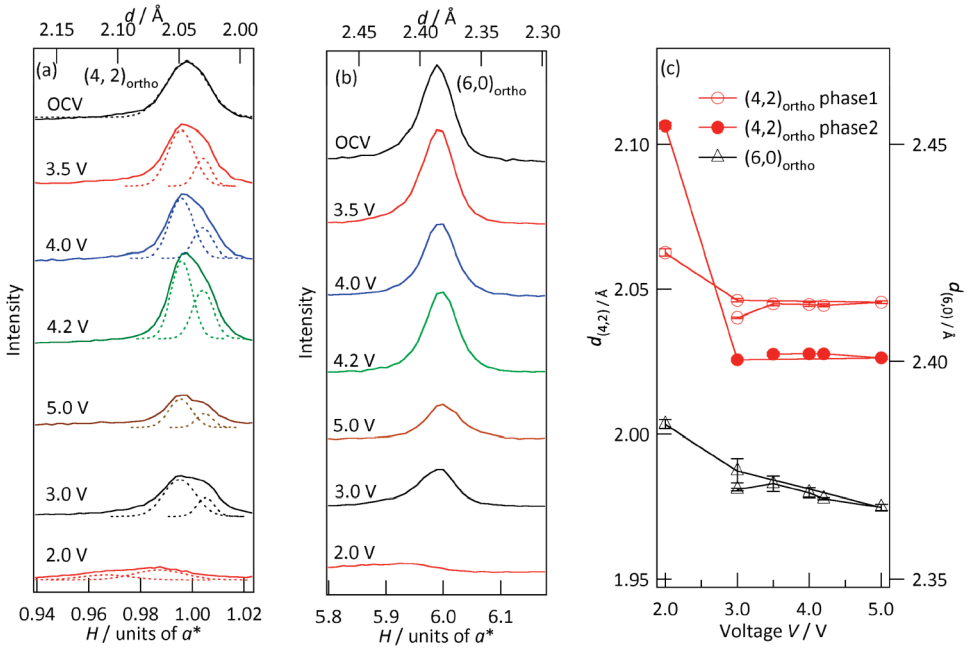

Figure 8. Surface XRD peaks of $(4,2)_{ortho}$ (a), $(6,0)_{ortho}$ (b) and voltage dependence of *d*-values (c) for $LiNi_{0.8}Co_{0.2}O_2$ (110) during anodic potential steps from 3.0 to 5.0 V and cathodic potential steps from 5.0 and 2.0 V.

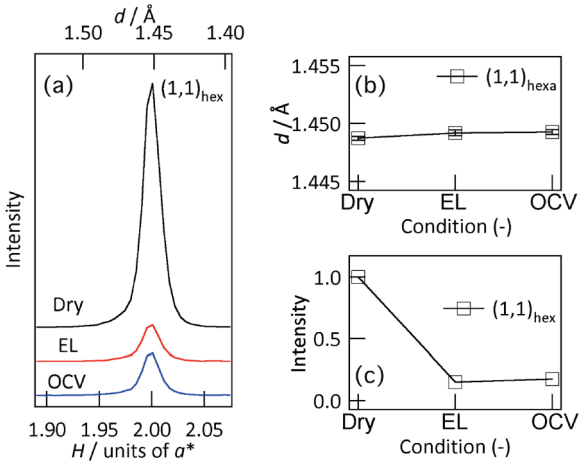

Figure 9. Surface XRD peak profiles (a), intensities (b) and d-values for $(1,1)_{hex}$ reflections of $LiNi_{0.8}Co_{0.2}O_2$ (003).

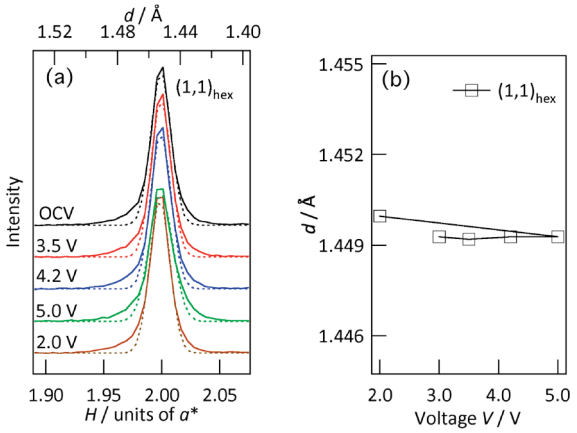

Figure 10. In-plane XRD peaks and voltage dependence of the *d*-values for the $(1,1)_{hex}$ peak of $LiNi_{0.8}Co_{0.2}O_2$ (003) with anodic potential steps from 3.0 to 5.0 V and cathodic potential steps from 5.0 and 2.0 V.

4.2 V, while a solid electrolyte interface (SEI) phase was observed on the cathode charged to 4.2 V and higher. The SEI contains electrolyte oxidation products such as dicarbonyl anhydride and polyester functionalities. It is believed that the SEI layer plays a key role in the calendar life of lithium batteries. Amine et al. observed surface structural changes after an accelerated aging test using X-ray absorption spectroscopy (XAS) and transmission electron microscopy (TEM) for $LiNi_{0.8}Co_{0.2}O_2$.[34] They observed a Li_xNi_1O-type layer on the particle and concluded that these surface layers were a significant contributor to the cathode impedance rise. However, these experimental systems based on polycrystalline electrodes have the following drawbacks for clarifying the electrode reaction mechanism. First, polycrystalline materials form a complex electrode/electrolyte interface that is influenced by many parameters such as surface structure, surface morphology, surface defects, and grain boundaries. Second, ex situ observations are limited to providing information on the electrode surface after a certain electrochemical reaction. Third, no structural information has been available for the electrode surface, where the reaction is initiated.

In the present study, the surface and bulk structural changes at the initial stage of the electrochemical process were determined for $LiNi_{0.8}Co_{0.2}O_2$ epitaxial thin films using a restricted lattice plane and the in situ surface XRD technique. Figure 11 schematizes the electrode reactions in $LiNi_{0.8}Co_{0.2}O_2$ thin films during the first charge/discharge process based on the present surface XRD and our previous XRR studies. X-ray surface scattering studies yield useful information about the surface structure that can elucidate the interfacial reaction mechanism under lithium intercalation fields. Bulk structural changes between 3.0 and 5.0 V provided direct evidence for 2D lithium diffusion

(34) Abraham, D. P.; Twesten, R. D.; Balasubramanian, M.; Petrov, I.; McBreen, J.; Amine, K. *Electrochem. Commun.* **2002**, *4*, 620.

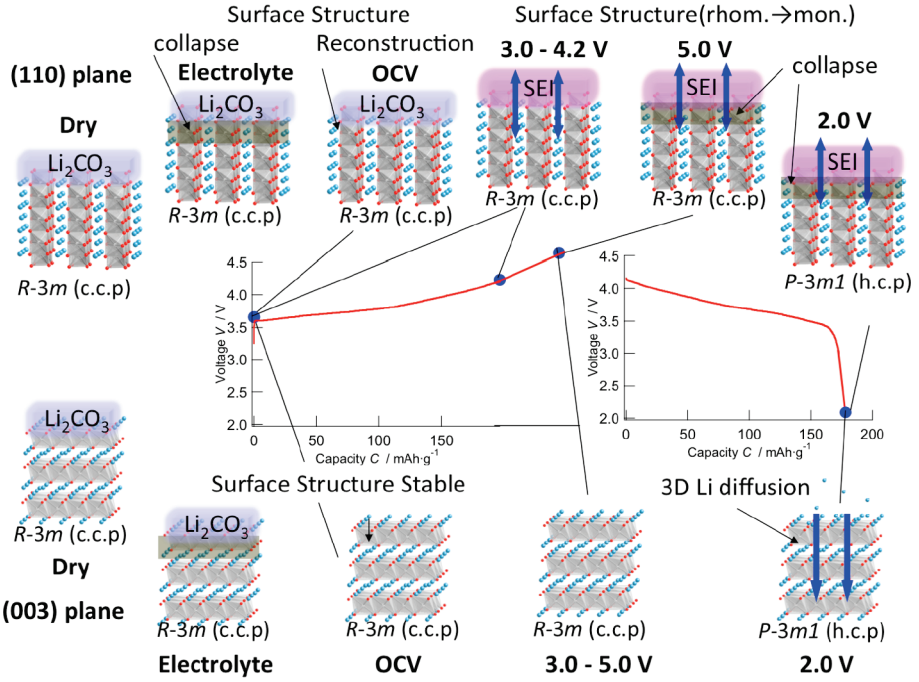

Figure 11. Schematic drawing of the $LiNi_{0.8}Co_{0.2}O_2$ during charge−discharge for the epitaxial films.

in the $LiNi_{0.8}Co_{0.2}O_2$ electrode: a (110) $LiNi_{0.8}Co_{0.2}O_2$ film with its infinite 2D $[(Co_{0.8}Ni_{0.2})O_6]_\infty$ plane perpendicular to the electrode/electrolyte interface showed intercalation activity, while a $LiNi_{0.8}Co_{0.2}O_2$ (003) film with its 2D plane parallel to the electrolyte showed no activity. These intercalation properties of the (110) and (003) films are consistent with the 2D nature of layered structures. Surface XRD studies confirm that the surface behaves rather differently from the bulk during the electrochemical process. The surface structures on both the (110) and (003) planes were partly destroyed in the electrolyte and reconstructed in the following process. The electric double layer formed by contact with the electrolyte might lead to surface reorientation and also a chemical reaction, such as dissolution of the surface impurity into the electrolyte and an ion exchange reaction. During the first electrochemical process, the (110) surface structure showed a transformation from rhombohedral to monoclinic, while no transformation was observed for the (003) plane. No phase transition to the cubic Li_xNi_1O phase, which has been detected by the TEM study,[34] was observed at the electrode surface. We focused on detecting the starting point of the reaction on electrode/electrolyte interface, while the TEM study observed the $LiNi_{0.8}Co_{0.2}O_2$ surface after an accelerated charge/discharge measurements from 40 to 70 °C. These experimental results clarified the structural changes of the electrode surface at the initial stage of the charge and discharge reactions and at the last stages of battery reaction after long-term charge−discharge experiments, which correspond to the deterioration mechanism.[35,36]

There is much knowledge about surface structural changes at ideal interfaces. For example, adsorption of oxygen on clean germanium surfaces brings about displacements of surface atoms from their normal bulk lattice positions.[29] Surface structural studies using these ideal surfaces have demonstrated that surface structures are reconstructed to lower the surface energy and are different from bulk structures. In the case of the solid/liquid interface, surface phase transitions of monolayer Bi electrodeposited on Au(111) single crystal were demonstrated using in situ X-ray surface scattering.[35] The surface structures at electrochemical interfaces are thought to change by adsorption species and significantly affect the electrode reaction. Similar to these ideal systems, the structural changes at the $LiNi_{0.8}Co_{0.2}O_2$/electrolyte interface were different from those of bulk: the deconstruction and reconstruction processes were observed in the initial reaction process. However, the electrode/electrolyte interfaces of lithium batteries involved not only adsorption of electrolyte species but also lithium diffusion, dissolution of impurities, and formation of SEI layer. It is therefore still difficult to interpret the surface structural changes observed using the epitaxial thin electrodes. The behavior observed in the case of $LiNi_{0.8}Co_{0.2}O_2$ is common to all intercalation electrodes. We observed the same behavior for $LiMn_2O_4$: the surface structure of $LiMn_2O_4$ drastically changed upon being soaked into the electrolyte and was gradually reconstructed under an applied voltage during the first charge process.[36] The reconstruction rate depends on the electrode material and may be related to the stability of the surface structure.

4. Conclusion

A new in situ experimental technique for detecting bulk and surface structural changes was developed for lithium battery intercalation electrodes using a restricted reaction

(35) Tamura, K.; Wang, J. X.; Adzic, R. R.; Ocko, B. M. *J. Phys. Chem. B* **2004**, *108*, 1992.

(36) Hirayama, M.; Sakamoto, K.; Mori, D.; Hiraide, T.; Yamada, A.; Sonoyama, N.; Tamura, K.; Mizuki, J.; Kanno, R., submitted for publication.

field for the electrochemical intercalation reaction and synchrotron XRD. The diffraction study indicated the orientation dependence of the intercalation mechanism for $LiNi_{0.8}Co_{0.2}O_2$ with its layered rocksalt structure. The (110) film showed structural changes upon Li (de)intercalation between 3.0 to 4.2 V, while the (003) film showed no structural change in this voltage range. However, the (003) film exhibited Li intercalation through the (003) surface at 2.0 V, which points to 3D lithium diffusion in the 2D structure. For the first time, the surface structure was successfully observed during the electrochemical intercalation process using an experimental technique combining surface XRD and epitaxial film electrodes. The (110) surface showed the collapse-reconstruction process, which is completely different from the bulk structural changes with Li (de)intercalation. The (003) surface is stable between 3.0 and 5.0 V. Our new experimental technique to detect the surface structure of lithium battery electrodes is promising for direct observation of interfacial phenomena between electrode and electrolyte and for obtaining information on stability for battery reactions.

Acknowledgment. This study was conducted in collaboration with the Genesis Research Institute. The work was partly supported by the Grant-in-Aid for Scientific Research (A), Japan Society for the Promotion of Science. The synchrotron radiation experiments were performed as projects approved by the Japan Synchrotron Radiation Research Institute (JASRI) (Proposal Nos. 2006A1663 and 2007A3628).

Note Added after ASAP Publication. Figure 4 and the Figure 5 caption were incorrect in the version published ASAP May 14, 2009; the corrected version was published ASAP May 22, 2009.